Investigation of the micro-mechanical properties of femtosecond laser-induced phases in amorphous silica

Christos-Edward Athanasiou*, Yves Bellouard
Galatea Lab, STI/IMT, Ecole Federale Polytechnique de Lausanne (EPFL), Rue de la Maladiere 71b, 2002-CH

ABSTRACT

Femtosecond pulses used in the regime where self-organized patterns are found have two noticeable effects in amorphous silica's (a-SiO_2) optical and chemical properties: The decrease of the material's refractive index as well as an enhanced etching selectivity. However, the effect on the material mechanical properties is unexplored. In this paper, we present elastic modulus measurements of fused silica exposed to femtosecond laser pulses in the regime where nanogratings are found. The measurement principle is based on the use of femtosecond laser fabricated displacement amplification mechanism combined with a discrete stiffness model. In this laser exposure regime, a significant decrease of the elastic modulus is observed. Our findings are consistent with the existence of a porous structure found within nanogratings lamellas. .

Keywords: silica, femtosecond laser, mechanical characterization, micromachining

1. INTRODUCTION

Femtosecond laser pulses interact in unusual ways with matter. In dielectrics, non-linear effects such as multiphoton absorption result in several forms of permanent modification[1] depending on the laser energy deposition on the material. In fused silica (the amorphous form of a-SiO_2) in particular, upon exposure to femtosecond pulses, three types of structural modification have been reported as a function of energy and pulse duration[2]. Type I, where continues modification take place[3], type II, where self-organized patterns consisting of 'nanogratings' are found[4] – this is the regime where this paper is focused on-, and type III where the ablation process starts[5].

Thanks to the use of fused silica in femtosecond laser machining[6,7], the chemical and optical properties of femtosecond laser-irradiated silica structures in the three types of regimes have been widely investigated. Nevertheless the mechanical properties of silica's femtosecond laser-induced structures still remain largely unexplored due to the inherent experimental difficulties associated with material testing in small scales. Our knowledge is restricted to the nanoindentation measurements performed by Y. Bellouard *et al.*, in type I regime, where a increase of the of the elastic modulus was reported[8].

In this paper, we present new insights on the mechanical behavior of femtosecond-laser irradiated fused silica in the type II regime. We do so, by using a femtosecond-laser machined amplification mechanism in conjunction with a simplified mechanical model to indirectly extrapolate the elastic modulus of the femtosecond laser-affected zones. A significant decrease in the elastic modulus of the material in this regime is reported. We further validate our findings by using the empirical Phani-Nuyogi relationship[9] to predict the elastic modulus of porous ceramic materials.

In the first part of the paper, we describe the fabrication and working principle of the displacement amplification mechanism as well as a simple mechanical model that links displacement measurements with elastic modulus of laser-affected zones. Later, we present and discuss our experimental results, mainly from the material science point of view.

2. DEVICE PREPARATION AND WORKING PRINCIPLE

2.1 Device design and fabrication

The device consists of a monolithic mechanism (shown in Fig. 1a,b) that includes a loading bar and an amplification stage to measure the elongation of the loading bar. It is fabricated using a two-step femtosecond laser-based process described in detail elsewhere[6,7]. The 250-μm thick silica substrate is first exposed to low-energy femtosecond laser pulses (275 fs pulses at 1030 nm emitted from an Yb-fiber amplifier operating at 800 kHz). The laser beam is focused using a 20- objective (OFR-20X-1054, Thorlabs, NJ, USA) with a numerical aperture (NA) of 0.40. As a result, the material structure is locally modified, resulting in an accelerated etching rate in laser-exposed regions[6,7]. The follow-up etching step is performed in a low concentration hydrofluoric HF bath (2.5 %) for twenty four hours.

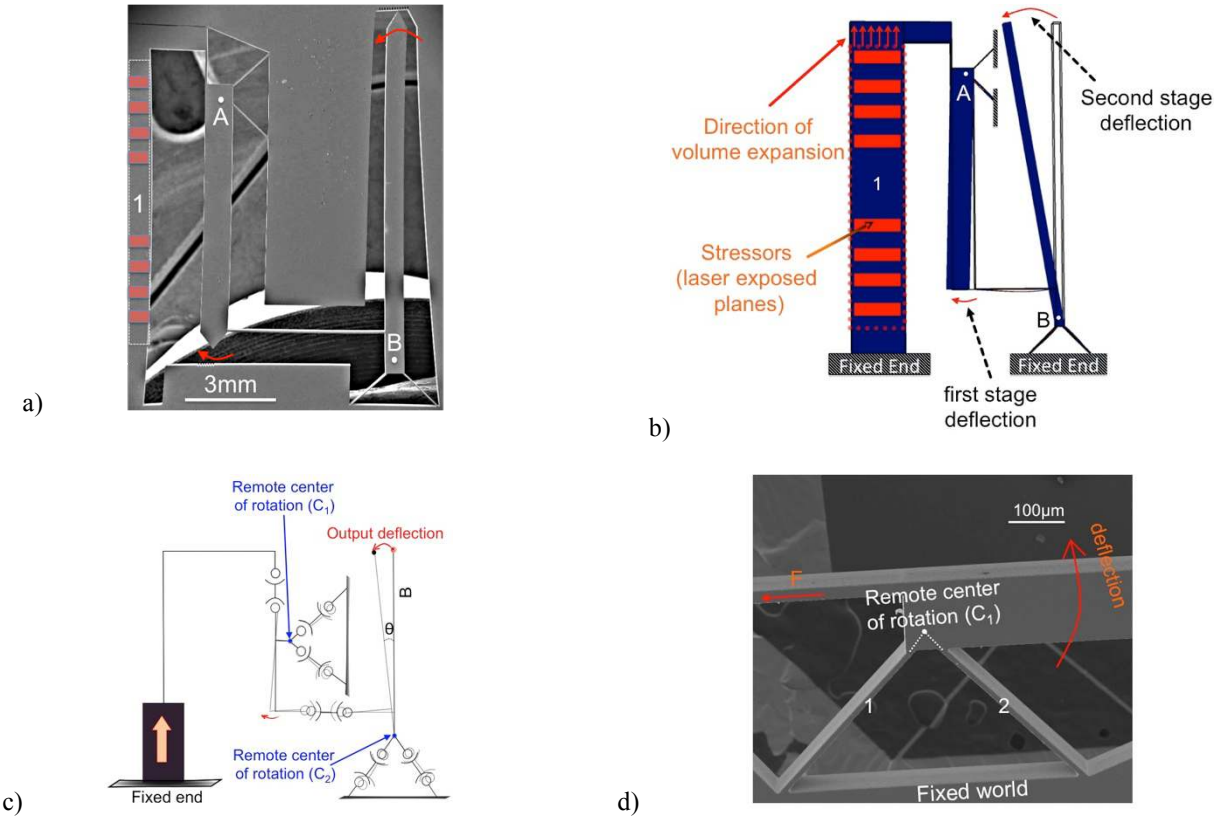

Figure 1. (a) Scanning electron microscope view of the displacement amplification mechanism. The red boxes in bar 1 represent the machined stressors. (b) A finite element analysis is illustrated for the deformed system. (c) Kinematics of the displacement amplification mechanism. The circles represent one-degree-of-freedom rotation pivot joints. The bars represent rigid links. The dash lines indicate the kinematics being operated. The end-effector is body B. (d) Scanning electron microscope view of part of the displacement amplification mechanism fabricated using femtosecond laser machining and chemical etching.

In another paper[10], we have demonstrated that femtosecond laser-affected zones in Type II modifications in silica exhibit a net volume expansion. We use this principle to expand the loading bar in a controlled manner by juxtaposing laser-affected zones consisting of lines written across the volume. We call these laser-affected structures, *'stressors'*.

To measure the loading bar's elongation resulting from the stressors machining, the displacement is mechanically amplified using a two-stage flexure-based lever mechanism connected in parallel to the main loading bar (Fig. 1a, bar 1). The lever amplification kinematics is illustrated using pivot joints (Fig. 1c). A lever pivots around a point (point C_1 in Fig. 1c,d) anchored to a fixed body. Two bars (bars 1 and 2 in Fig. 1d) fixed at their one end (from the kinematics point of view each bar is equivalent with two pivots) form a hinge, which is used to interface the linear motion of the loading bar with the angular motion of the pivot. The loading bar (Fig. 1a) forming the input of the mechanism is attached at one end while the output of the mechanism is at the other end of the lever (Fig. 1b). The second stage of the amplification acts exactly like the first one, scaling up the input linear motion even more. The amplification level for small angles θ of the end-effector bar (Fig. 1c) is simply the ratio of the output displacement of the mechanism and the input displacement induced in the system.

With the use of the same laser, yet at lower pulses energy, so that no further modification is made to the material, we measure the displacement of the end-effector of the amplification mechanism using the third harmonic optical signal generated while scanning the beam across the specimen's surface[11,12,13].

The displacement of the amplification mechanism is linked to the elastic modulus of the stressors through the stiffness model described in the next paragraph.

2.2 Modeling the loading bar

In this section, we link the behavior of the *elongation of the loading bar* with the *elastic modulus of the stressors.*

The stressors are implemented by scanning adjacent lines with a writing speed of 10 mm/s and with energy per pulse of 220 nJ so that Type II modification is taking place while having a volume variation as high as possible[10].

The stressors induce an overall expansion of the loading bar. The volume exposed to the laser is inhomogeneous and consists of a composite structure of modified (which consist of a arrangement of periodic nanoplanes) and unmodified zones[14]. As a first approximation, we model the sidebars under loading as a spring arranged in parallel with the elongated laser-affected zone as shown in Fig. 2a. We express k_2 as the laser-affected volume and k_1 as the stiffness of the non-affected sidebars. This model is a simplification since it does not take into account interfacial energy between the various domains (laser affected, pristine, etc.). Nevertheless, it provides a first insight - reasonably accurate - of the mechanical behavior of the ensemble[15].

If n is the number of stressors machined in the system, the total stiffness variation is simply the addition of the two parallel stiffness's (as shown in Fig. 2b) of the springs k_1 and k_2 and is given by the following equation:

$$Stiffness = E_{SiO_2}\frac{a_1 b_1 - a_0 b_0}{nt} + E_{LaserAffectedZone}\frac{a_0 b_0}{(n-1)t} \quad (1)$$

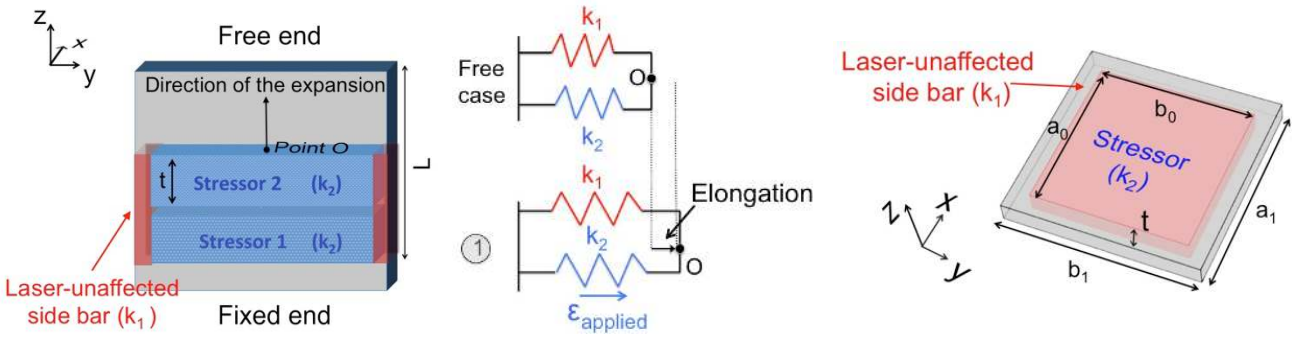

Figure 2. (a) 2D visualization of the loading process during the writing of the stressors. The mechanical energy that develops due to the localized material expansion, results in the principal loading of the sidebars. (b) Simplified spring model of the loading process. (c) Parameters used to describe a single stressor.

In this model, we make the following assumptions:

1/ The laser-written structures are treated as 'homogenized', in other words, we neglect fine structures like nanogratings, but consider it as a homogeneous material, albeit of lower density than the pristine material. For the analysis we choose different values for the elastic modulus of the laser-affected zones as indicated later, in Fig. 3b.

2/ The shear stress that is transferred from the laser-affected zone to the pristine fused silica is considered low and negligible.

3. EXPERIMENTAL RESULTS

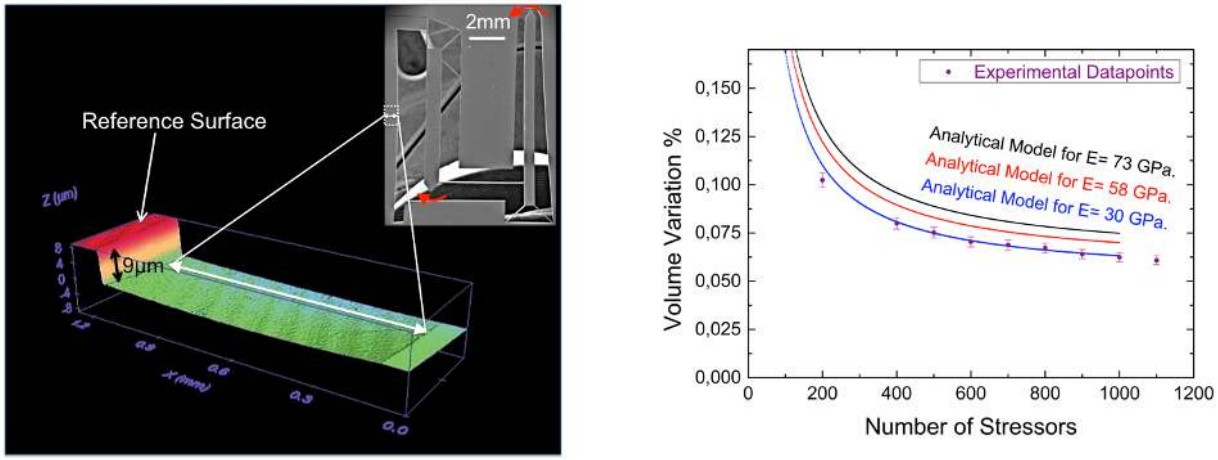

Figure 3. (a) Using white light interferometry for measuring the profile of the deformed device, a significant volume variation was found and attributed to out-of-plane motion. (b) Analytical model for different values of elastic modulus for

the laser-affected zones and experimental data of the induced volume variation in the device. The experimental data were corrected with the measured factor of out-of-plane motion displacement of the device.

As illustrated in Fig. 3a, we observed an out-of-plane motion of the system. The profile of the loading bar (bar 1 in Fig. 1a) revealed that 60 % of the induced volume variation in the system was allocated to undesired out-of-plane displacement. As illustrated in Fig. 3b, by correcting the experimental data for the out-of-plane factor, we find that the measured volume variation and the one predicted by the analytical model matches rather well for lower estimated values of the elastic modulus of laser affected zones. This observation is consistent with the existence of less dense material in laser-affected zones formed of nanogratings. Indeed, J. Canning *et al.* reported on the presence of a porous structure[14]. The porous material supports a lower refractive index[16] (itself consistent with a lower density material) and in turn a possible significant decrease of elastic modulus.

$$E_{porous} = E_0 \left(1 - \frac{p}{p_c} \right)^f \tag{2}$$

The elastic properties of porous materials can be predicted by the empirical relationship of Phani and Nuyogi for ceramic materials[9]:

where E_{porous} is the effective elastic modulus of the porous material with porosity p, E_0 is the elastic modulus of solid material, p_c is the porosity at which the effective elastic modulus becomes zero and f is the parameter dependent on the pore geometry[9]. From the images by the work of Canning *et al.*, the pores in the laser-affected zones are of complex shapes and interconnected[14]. Based on these images, we estimate the porosity of the zones to range between 0,4 - 0,5. The value of the characteristic exponent f is for almost all the investigated materials in the range of 1,10 - 1,70[17].

Porous materials with high concentration in surface inhomogeneities and cracks have a low value of this parameter. Here, as an example we will use a conservative value (f = 1,20). Finally, as noted by Wagh *et al.* fittings of experimental data for different materials[18] give approximately $p_c = 1$ and this is the value we adopt for this example.

Indeed, as indicated in Table 1, the values found for the different cases of porosity validate the above discussion of the decreased elastic modulus of the laser-affected zones.

Elastic modulus of laser-affected zones for different porosity parameters	p = 0,40	p = 0,45	p = 0,50
E_{porous} (GPa.)	**41,1**	**37,8**	**34,0**

Table 1. Estimation of the laser-affected zones elastic modulus of the using the Phani-Nuyogi empirical relationship for ceramic materials[9].

4. CONCLUSION AND DISCUSSION

In this paper, we presented our preliminary results on the mechanical behavior of femtosecond laser affected zones in pristine fused silica matrix in the regime where nanogratings are formed (type II). In particular, a significant decrease on the elastic modulus is reported. The measurements are consistent to the porous structures that the nanogratings

consist of. The relationship of Phani and Nuyogi to predict the elastic modulus of the stressors validates the findings of a decreased elastic modulus.

In parallel, we demonstrate that a femtosecond laser machined displacement amplification mechanism along with a simple stiffness model are adequate to provide indirect -yet reliable- first order measurements of the elastic modulus of a femtosecond laser machined planes (what we call as stressors). We should note that for the sake of simplicity the stressors are considered as a homogeneous material and interfacial effects are not taken into account.

Nevertheless, another important parameter neglected in this work, the one of the internal stresses developed within and very close to the stressors. Bellouard *et al.* have reported on path-dependent phenomena[19] in the writing sequence of stressors due to the gradual built-up of internal stresses as the scanned lines are placed close enough one to another (Fig. 4).

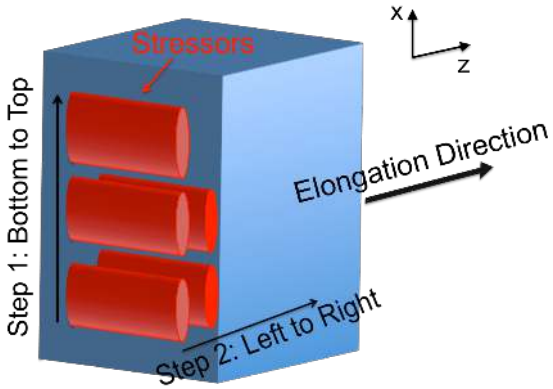

Figure 4. The writing strategy of the stressors machining along the loading bar is illustrated. Due to the built-up of internal stresses during the machining process the writing strategy plays a key role to the microstructure of the material that is formed and eventually its elastic modulus.

For a more comprehensive understanding of the mechanical behavior of the femtosecond laser-affected zones in the type II regime, an instrument particularly developed to study the mechanics of the laser-affected zones, a micro-tensile tester will be used in the future[15].

REFERENCES

[1] Bloembergen, N., "Laser-induced electric breakdown in solids," IEEE J. Quant. Electron. 10(3), 375–386 (1974).

[2] Hnatovsky, C., Taylor, J. R., Rajeev, P. P.,Simova, E.,Bhardwaj, V. R., Rayner, D. M. and Corkum, P. B., "Pulse duration dependence of femtosecond-laser-fabricated nanogratings in fused silica," Appl. Phys. Lett. 87(1), 014104 (2005).

[3] Davis, K. M., Miura, K., Sugimoto, N. and Hirao, K., "Writing waveguides in glass with a femtosecond laser," Opt. Lett. 21(21), 1729–1731 (1996).

[4] Shimotsuma, Y., Kazansky, P. G., Qiu, J. R. and Hirao, K., "Self-organized nanogratings in glass irradiated by ultrashort light pulses," Phys. Rev. Lett. 91(24), 247405 (2003).

[5] Glezer, E. N. and Mazur, E., "Ultrafast-laser driven micro-explosions in transparent materials," Appl. Phys. Lett. 71(7), 882–884 (1997).

[6] Marcinkevičius, A., Juodkazis, S., Watanabe, M., Miwa, M., Matsuo, S., Misawa, H. and J. Nishii, "Femtosecond laser-assisted three-dimensional microfabrication in silica," Opt. Lett. 26(5), 277–279 (2001).
[7] Bellouard, Y., Said, A., Dugan, M. and Bado, P., "Fabrication of high-aspect ratio, micro-fluidic channels and tunnels using femtosecond laser pulses and chemical etching," Opt. Express 12(10), 2120–2129 (2004).
[8] Bellouard, Y., Colomb, T., Depeursinge, C., Dugan, M., Said, A. A. and Bado, P., "Nanoindentation and birefringence measurements on fused silica specimen exposed to low-energy femtosecond pulses," Opt. Express 14(18), 8360–8366 (2006).
[9] Phani, K. K. and Niyogi, S. K., "Young's modulus of porous brittle solids," J. Mater. Sci. 22(1), 257-263 (1987).
[10] Champion, A. and Bellouard, Y., "Direct volume variation measurements in fused silica specimens exposed to femtosecond laser," Opt. Mater. Express 2(6), 789-798 (2012).
[11] Barad, Y., Eisenberg, H., Horowitz, M. and Silberberg, Y., "Nonlinear scanning laser microscopy by third harmonic generation," Appl. Phys. Lett. 70(8), 922 (1997).
[12] Müller, M., Squier, J., Wilson, K. R. and Brakenhoff, G. J., "3D microscopy of transparent objects using third harmonic generation," J. Microsc. 191(3), 266–274 (1998).
[13] Athanasiou, C. E., McMillen, B. W. and Bellouard, Y., "A monolithic micro-tensile tester for investigating silica micromechanics, fabricated and fully operated using a femtosecond laser," CLEO:2014, AW1H.6 (2014).
[14] Canning, J., Lancry, M., Cook, K., Weickman, A., Brisset, F. and Poumellec, B., "Anatomy of a femtosecond laser processed silica waveguide," Opt. Mater. Express 1(5), 998–1008 (2011).
[15] Athanasiou, C. E. and Bellouard, Y., "A monolithic micro-tensile tester for investigating silicon dioxide polymorph micromechanics, fabricated and operated using a femtosecond laser," Micromachines 6(9), 1365-1386 (2015)
[16] Bricchi, E., Klappauf, B. G. and Kazansky, P. G., "Form birefringence and negative index change created by femtosecond direct writing in transparent materials," Opt. Lett. 29(1), 119–121 (2004).
[17] Kovacik, J., "Correlation between the Young's modulus and the porosity of porous materials," J. Mater. Sci. Lett. 18(3), 1007-1010 (1999).
[18] Wagh, A. S., Poeppel, R. B. and Singh, J. P. "Open pore description of mechanical properties of ceramics," J. Mater. Sci. 26(14), 3862-3868 (1991).
[19] Bellouard, Y., Said, A. A., Dugan, M. and Bado, P., "On the role of scanning line sensitivity on the etching of fused silica specimens exposed to femtosecond laser pulses," Proc. SPIE 8247, 82470T (2012).